 doi:10.20944/preprints202103.0205.v1

Article

Soluble epoxide hydrolase inhibition ameliorates phenotype and cognitive capabilities in a murine model of Niemann Pick disease type C

Christian Griñán-Ferré[1], Júlia Companys-Alemany[1], Júlia Jarné-Ferrer[1], Sandra Codony[2], Célia González-Castillo[3], Daniel Ortuño-Sahagún[4], Lluïsa Vilageliu[5,6,7], Daniel Grinberg[5,6,7], Santiago Vazquez[2], Mercè Pallàs[1]

[1] Pharmacology and Toxicology Section and Institute of Neuroscience. Faculty of Pharmacy and Food Sciences. University of Barcelona, Av. Joan XXIII, 27-31, 08028 Barcelona, Spain.
[2]Laboratory of Medicinal Chemistry (CSIC, Associated unit), Faculty of Pharmacy and Food Sciences and Institute of Biomedicine (IBUB), University of Barcelona, Av. Joan XXIII, 27-31, 08028 Barcelona, Spain.
[3]Tecnológico de Monterrey, Escuela de Medicina y Ciencias de la Salud, Campus Guadalajara. Zapopan, Jalisco, México.
[4]Laboratorio de Neuroinmunobiología Molecular, Instituto de Investigación en Ciencias Biomédicas (IICB), Centro Universitario de Ciencias de la Salud (CUCS), Universidad de Guadalajara, Jalisco, México.
[5]Department of Genetics, Microbiology and Statistics, Faculty of Biology, University of Barcelona, 08028 Barcelona, Spain.
[6]Institut de Biomedicina de la UB (IBUB)-Institut de Recerca Sant Joan de Déu (IRSJD), 08028 Barcelona, Spain.
[7]Centre for Biomedical Research on Rare Diseases (CIBERER), 08028 Barcelona, Spain.

* Correspondence:
e-mail: pallas@ub.edu
Pharmacology and Toxicology Section and Institute of Neuroscience. Faculty of Pharmacy and Food Sciences. University of Barcelona, Av. Joan XXIII, 27-31, 08028 Barcelona, Spain.

Abstract: Niemann-Pick type C (NPC) disease is a childhood autosomal recessive inherited rare neurodegenerative disease, characterized by the accumulation of cholesterol and glycosphingolipids, implicating the autophagy-lysosome system. Inhibition of soluble epoxide hydrolase (sEH), an enzyme that metabolizes epoxy fatty acids (EpFAs) to 1,2-diols, exerts beneficial effects in modulating inflammation and autophagy, critical features of the NPC disease.

This study aimed to evaluate the effects of UB-EV-52 a sEH inhibitor (sEHi) in the Npc mouse model by administering for 4 weeks (5 mg/kg/day). Behavioral and cognitive assays (open field test (OF), elevated plus maze (EPM), novel object recognition test (NORT) and object location test (OLT) demonstrated that treatment produced an improvement in short- and long-term memory as well as in spatial memory.

Moreover, the treatment with UB-EV-52 increased body weight and the lifespan by 25% and reduced gene expression of the inflammatory markers (i.e. *Il-1β* and *Mcp1*) and improved oxidative stress (OS) markers (*iNOS and Hmox1*) in the treated Npc mice group. Regarding the autophagic markers, we surprisingly found significantly reduced levels of the ratio LC3B-II/LC3B-I and a significant reduction of brain protein levels of lysosomal-associated membrane protein-1 (LAMP-1) in Npc mice treated group compared to non-treated. Lipid profile analysis showed a significant reduction in lipid storage in the liver and some slight changes in brain tissue in treated Npc mice compared to non-treated groups. Thus, Our results suggest that the pharmacological inhibition of sEH ameliorates most of NPC's characteristic traits in mice, demonstrating that sEH can be considered a potential therapeutic target for this condition.

Keywords: Niemann-Pick type C; soluble epoxide hydrolase; autophagy; cognitive decline; lifespan; inflammation; cholesterol; sphingolipids.

1. Introduction

Niemann Pick disease type C (NPC, MIM # 257220) is a rare (1/120,000 live births in Europe) neurodegenerative, autosomal recessive disease. The disorder is characterized by a lipid trafficking defect that causes an inability to process cellular cholesterol, accompanied by secondary accumulation of glycosphingolipids in affected individuals' lysosomes [1,2]. It is caused by mutations in the NPC1 (this occurs in 95% of the diagnosed cases) or in the NPC2 genes [3]. NPC1 is a late-endosomal transmembrane protein, which binds cholesterol, while NPC2 resides in the lysosomal lumen and transfers cholesterol to NPC1 [4]. Therefore, defects in NPC1 or NPC2 proteins lead to the accumulation of cholesterol and glycosphingolipids in lysosomes and cause hepatic, pulmonary and neuropsychiatric disorders in humans [4–6]. NPC's first clinical manifestations appear during childhood and are typically diagnosed before 10 years of age. Patients often present with cerebellar ataxia, progressive behavioral and cognitive disabilities, as well as dementia [5]. Adult manifestation (from 15 years) is rare, the progression is usually much slower, and patients present a broad phenotypic spectrum similar to childhood manifestation, including epilepsy and parkinsonism syndrome. Besides, the disease's progression and life expectancy are causally related to the appearance of neurological symptoms [5]. Cellular and molecular hallmarks in the central nervous system (CNS) are the presence of lipids inclusions, changes in lipid content composition, increased storage of cholesterol and multiple sphingolipids in neuron membranes [7]. These changes in the NPC brain are accompanied by mitochondrial dysfunction, oxidative stress (OS) and a robust inflammatory component (gliosis in grey and white matter, microglial activation) that finally lead to synaptic disruption phenomena throughout the brain [4,8].

Moreover, protein misregulation is also present in NPC tissues. Gene expression analysis from patients with NPC revealed molecular similarities with neurodegenerative diseases, such as the accumulation of hyperphosphorylated tau in neurofribillary tangles (NTFs) and abnormal processing of β-amyloid [9,10]. Cells have different, efficient mechanisms to eliminate damaged organelles, aberrant proteins aggregation and other wastes produced by cell functioning in normal or pathological situations. Autophagy is one of those mechanisms that implicate a large control of lysosome-mediated functions [11]. The autophagic process is necessary for maintaining cellular homeostasis and cell survival, especially under amino acid starvation or cellular stress. Besides, autophagy is necessary for normal CNS development and function [12]. It has been implicated in most neurodegenerative diseases and other human diseases, such as cardiovascular diseases, immunological disorders, or cancer [13]. It is well-known that many factors affect the autophagic process in the brain, including inflammation, OS, synaptic plasticity alterations and aberrant accumulation of lipid metabolites. In NPC disease, autophagy induction was reported through increased vacuoles and accumulation of lipidated LC3 [14].

Moreover, it is established that the class III-PI3K/Beclin-1 complex is the key factor implicated in the induction of autophagy in NPC1 deficiency because its expression is mildly elevated in NPC1 deficient mouse tissue and human fibroblasts. Besides, Beclin-1 knockdown by siRNA decreases long-lived protein degradation [15]. Hence, the NPC disease's etiopathogenesis is mainly associated with aberrant cholesterol storage accumulation and two mainly altered inflammation and autophagy.

Successful therapy for NPC disease has been elusive up to now with modest results in motor and cognitive affectation by different strategies including miglustat [16], hydroxypropyl beta-cyclodextrins (HPßCD) [17] or anti-inflammatory drugs [18]. A combined therapy using HPßCD, allopregnanolone and miglustat has been shown to delay disease onset and to increase the lifespan of NPC1 mice by reducing intraneuronal lipid storage and positively influenced motor dysfunction [19]. The positive effect of miglustat mon-

otherapy was further improved by additional dual therapy with curcumin and miglustat and triple combination therapy [20]. A modest, but not negligible, cyclodextrins positive action and miglustat have been described in humans. Unfortunately, specific and effective treatment is not available at the moment. Thus, identifying promising therapeutic and preventive strategies for this condition has, so far, been challenging.

The enzyme soluble epoxide hydrolase (sEH; EC 3.3.2.10) is emerging as a pharmacological target because its inhibition has shown beneficial effects in metabolic disorders [21] and neurodegenerative diseases such as Alzheimer's disease (AD) [22,23] and Parkinson's disease (PD) [24]. In the arachidonic acid (AA) cascade, cytochrome P450 epoxygenases convert AA in epoxyeicosatrienoic acids (EETs), which are hydrolyzed by sEH into their corresponding dihydroxyicosatrienoic acids (DHETs) (DHETs) [25]. EETs are potent cellular signalling molecules regulating key events, such as improving mitochondrial dysfunction [26], reducing apoptosis [27], modulating autophagic response [28] and reducing inflammation [29]. Furthermore, EETs modulate specific processes in neuronal and glial cells, as well as the communication between different cell types [23]. Blocking sEH reduces the deleterious effects of ischemic stroke and subarachnoid haemorrhage [30]. Moreover, sEH inhibition reduces cognitive impairment in AD mice models, reducing OS, endoplasmic reticulum (ER) stress and, importantly, reducing neuroinflammation mediators such as tumour necrosis factor (TNF-α) and interleukin 1 beta (IL-1β) [22]. Finally, it has been recently described that 14,15-EETs reduces cholesterol accumulation in human fibroblasts from NPC patients, reducing cholesterol synthesis and improving autophagic flow [31].

As aforementioned, despite the research conducted for a useful treatment for NPC disease, a successful therapeutic tool has not been identified. Thus, anti-inflammatory, anti-oxidant or more specific drug to improve the prognosis for NPC patient can be a new insight [8]. In the current study, we demonstrated that using sEH as a target for fighting against this devastating disease can be a new starting point for developing NPC disease therapies. To this end, we tested a well-characterized sEHi (UB-EV-52) in a mouse model of the disease [31], which can inhibit the sEH at the brain level through an *in vivo* thermal shift assay (CETSA) [22], demonstrating the target engagement. Then, we focused our effort on the disease's hallmarks such as cognition, survival, changes in lipid accumulation, neuroinflammation, OS, synaptic plasticity and autophagic process activation.

2. Results

2.1.Changes in body weight and survival after UB-EV-52 treatment.

The body weight was measured weekly during the intervention. Starting from baseline (1 week of age), the Npc mice were significantly lower compared to Wt mice, whereas UB-EV-52 treatment significantly increased body weight in Npc mice (Fig 1C). Besides, as expected, the treatment did not modify Wt animals' average body weight increase, being 8.81 g for Wt Control group and 8.73 g for Wt treated group (Fig 1D). In contrast, a clear tendency to increase the average body weight increase of Npc treated (10.22 g) compared to the Npc Control group (8.84 g) (Fig 1D).

Significantly, sEHi treatment delayed Npc mice mortality compared to untreated animals, as shown in the Kaplan-Meier survival curve presented in (Fig 1D). Consequently, UB-EV-52 increased by 25% of the Npc lifespan (Fig 1E).

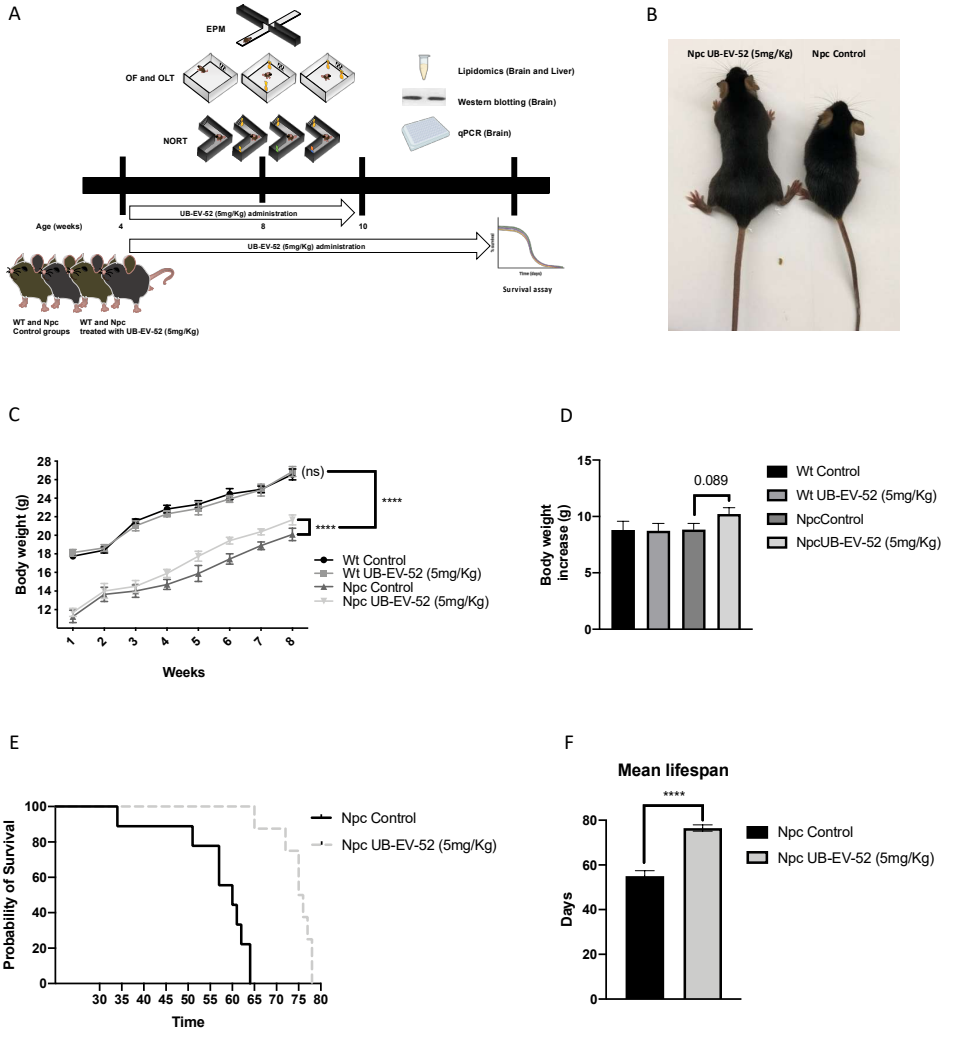

Figure 1. Scheme of experimental design **(A)**, Mouse phenotype **(B)**, Results of body weight curve in both females and males **(C)**, Results of total body weight increase in both females and males **(D)**, Survival curve in both females and males **(E)**, Mean lifespan in both females and males **(F)**. Values represented are mean ± Standard error of the mean (SEM); n = 48 (Wt Control n = 12, Wt UB-EV-52 (5mg/Kg) n = 12, Npc Control n = 12, and Npc UB-EV-52 (5mg/Kg) = 12). *p<0.05; **p<0.01; ***p<0.001; ****p<0.0001.

2.2.Sphingolipid and cholesterol profiling in mouse tissues and the effect of UB-EV-52 treatment.

To evaluate the effect of sEH inhibition in Npc and Wt mice on lipid storage, a relevant phenotype observed in NPC patients, brain and liver sphingolipid levels and cholesterol amounts were determined by gas chromatography-mass spectrometry.

As expected, significant differences were observed between Wt and Npc mice. Concretely, Npc animals showed a significant accumulation of sphingomyelin, dihydrosphingomyelin, ceramides and gangliosides (GM2 and GM3) (Supplementary Figs 1-2). Significant accumulation of cholesterol in the liver and brain of Npc mice was observed, compared to the Wt group (Supplementary Figs 1C-2C). Nevertheless, results showed that UB-EV-52 modified the lipid storage profile subtly in the brain from treated animals (Supplementary Fig 1). In the liver, a slight decrease in the evaluated lipid species was found (Supplementary Fig 2), which reached statistical significance only for dihydrosphingomyelin (Supplementary Fig 2C).

 doi:10.20944/preprints202103.0205.v1

2.3.Improvement in behavioral performance after UB-EV-25 treatment.

Locomotor activity was analyzed after UB-EV-52 treatment in the open field test (OFT) paradigm. The obtained results showed that Npc mice presented a diminution in locomotor activity as demonstrated by the significant diminution in the distance travelled compared to the Wt group (Fig 2A). Moreover, Npc mice remained more time in the center of the arena compared to the Wt group. They presented a decrease in vertical activity, quantified by the number of rearings, indicating a disease-associated limitation on its activity (Fig 2C). UB-EV-52 did not modify the locomotor activity in Wt mice while improved both parameters: the distance travelled and the time in the center for Npc mice, confirming an important change in this NPC disease characteristic trait (Fig 2A). Additional parameters measured in the OFT are presented in Table S1.

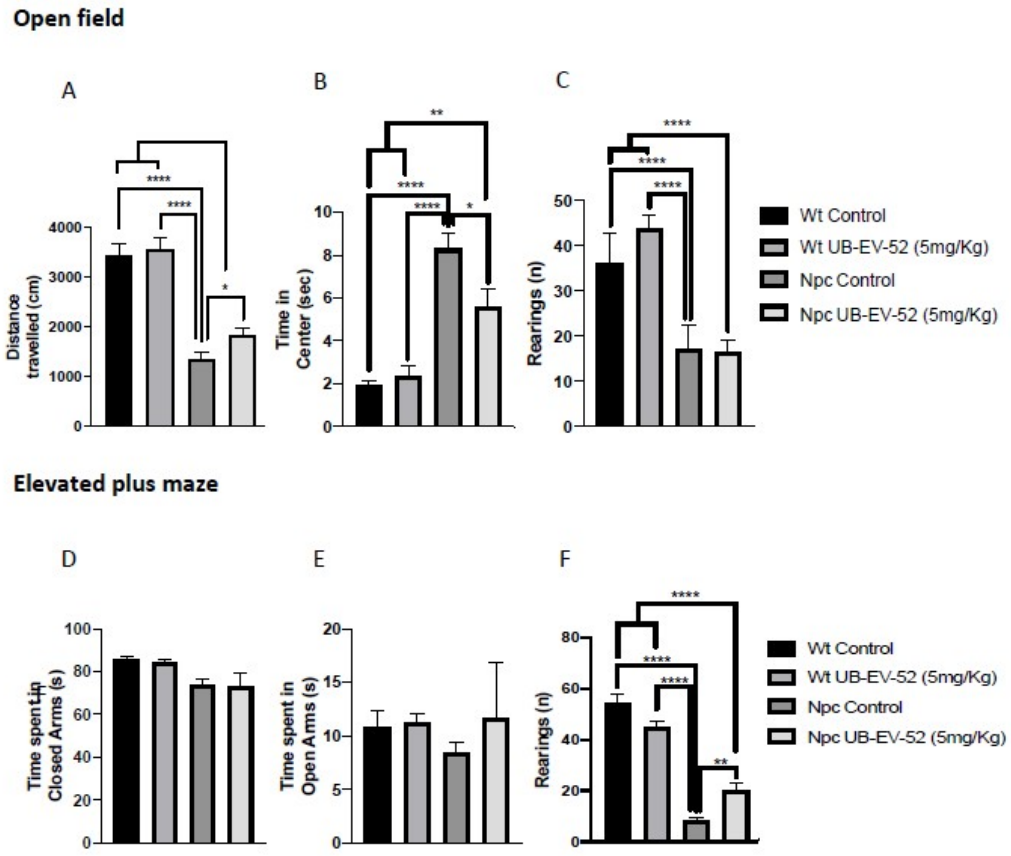

i

Figure 2. Results of OFT: Distance travelled in both females and males **(A)**, Time spent in Center zone **(B)**, Rearings **(C)**. Results of EPM: Time spent in Open Arms **(D)**, Time spent in Closed Arms **(E)**, Rearings **(F)**. Values represented are mean ± Standard error of the mean (SEM); n = 48 (Wt Control n = 12, Wt UB-EV-52 (5mg/Kg) n = 12, Npc Control n = 12, and Npc UB-EV-52 (5mg/Kg) = 12). *p<0.05; **p<0.01; ****p<0.0001.

Regarding anxiety-like behaviour, we studied several parameters by using an elevated plus maze (EPM). The result showed no significant changes neither for the phenotype nor for treatment conditions in comparison with the time spent by mice in open or closed arms at the age studied (Figs 2D-2E). Conversely, reduced vertical activity in

 doi:10.20944/preprints202103.0205.v1

this maze was observed for the Npc group compared to the Wt group, as well as a significant recovery in UB-EV-52 treated animals (Fig 2F). Additional parameters measured in the EPM are presented in Table S2 (Supplementary material).

2.4.Effect of UB-EV-52 treatment on cognitive capabilities in Npc mice.

The novel object recognition test (NORT) was used to assess cognitive performance after UB-EV-52 treatment. This test has been used previously in the Npc mouse model to prove cognitive impairment [31]. NORT was performed at 8 weeks of age, and analysis demonstrated that Npc showed reduced discrimination index (DI) compared to age-matched Wt mice at 2h or 24h test (Figs 3A-B). However, the Npc group treated with UB-EV-52 exhibited significantly reduced cognitive deficits in both short- and long-term memories determined for their Npc littermates. Those results demonstrated the beneficial effects on cognition after pharmacological inhibition of sEH, restoring it to a level similar to the Wt phenotype (Figs 3A-B).

Additionally, the object location test (OLT) paradigm was used to assess spatial memory. Results reinforced the results on NORT and denoted a significant spatial memory impairment in Npc in comparison with Wt mice. Furthermore, Npc mice treated with UB-EV-52 presented a higher exploration time for the new object location, pointing out an improvement in spatial cognitive capabilities after sEHi treatment (Fig 3C).

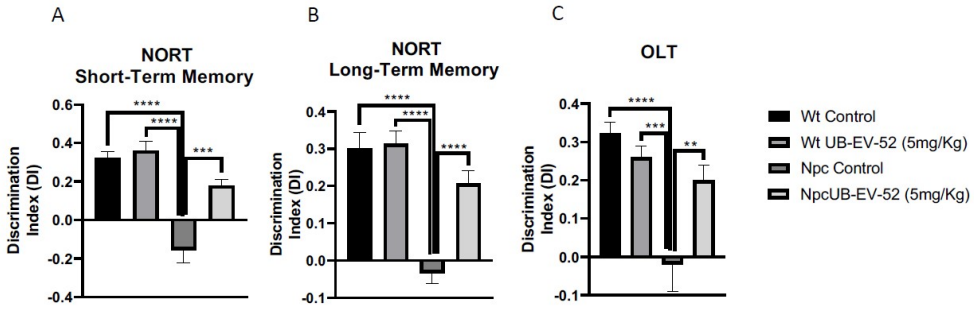

Figure 3. Results of NORT for short-term memory in both females and males **(A),** and long-term memory **(B)**. Results of OLT **(C)**. Values represented are mean ± Standard error of the mean (SEM); n = 48 (Wt Control n = 12, Wt UB-EV-52 (5mg/Kg) n = 12, Npc Control n = 12, and Npc UB-EV-52 (5mg/Kg) = 12) Discrimination index (DI). **p<0.01; ***p<0.001; ****p<0.0001.

2.5.Reduction of neuroinflammatory and oxidative stress markers after treatment with UB-EV-52 in Npc mice.

As expected, mutant mice presented a highly inflammatory profile with increases in several pro-inflammatory cytokines such as *Il-1β and Tnf-α* in comparison with Wt mice (Figs 4A-B). Furthermore, we went through other neuroinflammatory markers such as *monocyte chemoattractant protein 1 (Mcp1)* and the brain tissue astroglial marker *glial fibrillar acidic protein (Gfap)*, which are significantly increased in Npc mice (Figs 4C-D). Likewise, an important reduction in *Il-1β* and *Mcp1*, between Npc mice treated with UB-EV-52 compared to untreated littermate mice was determined (Figs 4A-C). Last, a clear tendency to decrease *Tnf-α* gene expression was observed in Npc mice treated with UB-EV-52 compared to untreated littermate mice. Although it did not reach significance, it is worth highlighting the extent of reducing Wt levels (Fig 4B).

To address the oxidative scenario in Npc mice, we evaluated the gene expression of *heme oxygenase decycling 1 (Hmox1)* and *inducible nitric oxidase (iNOS)*. Both enzymes are

 doi:10.20944/preprints202103.0205.v1

associated with OS state. We found a decreased *Hmox1* gene expression in Npc mice compared to Wt, which was reversed under UB-EV-52 treatment. Likewise, decreased levels of *iNOS* were present in the Npc group compared to the Wt group and were partially reverted in Npc treated animals (Figs 4E-F).

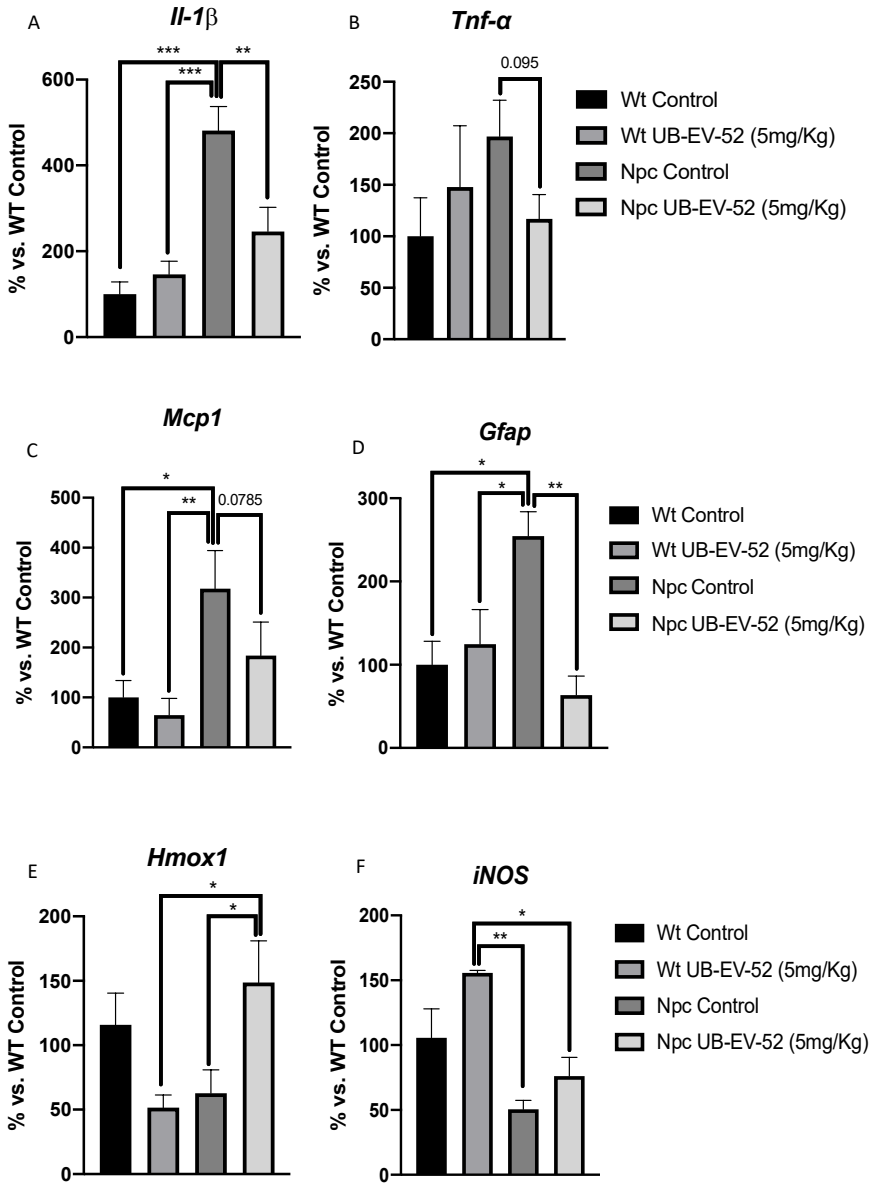

Figure 4. Gene expression of the inflammatory markers *Il1-β* **(A)**, *Tnf-α* **(B)**, *Mcp1* **(C)**, *Gfap* **(D)**, *Hmox1* **(E)** and *iNOS* **(F)** from brain tissue in both females and males. Gene expression levels were determined by real-time PCR. Values in bar graphs are adjusted to 100% for gene expression of Wt Control group. Values represented are mean ± Standard error of the mean (SEM); n = 24 (Wt Control n = 6, Wt UB-EV-52 (5mg/Kg) n = 6, Npc Control n = 6, and Npc UB-EV-52 (5mg/Kg) = 6).*p<0.05; **p<0.01; ***p<0.001.

Preprints (www.preprints.org) | NOT PEER-REVIEWED | Posted: 5 March 2021 doi:10.20944/preprints202103.0205.v1

2.6.Decreased autophagic markers and increased synaptic markers promoted by UB-EV-52 treatment in Npc mice.

The autophagic process was studied by Beclin-1, microtubule-associated proteins 1A/1B light chain 3B (LC3B) and lysosome-associated membrane glycoprotein 1 (LAMP-1) protein levels. Results showed that Npc mice presented a higher Beclin-1, LCB-II/I ratio and LAMP-1 protein levels than Wt littermates (Figs 5A-C, G). Furthermore, when mice were under UB-EV-52 treatment, a diminution in Beclin-1, LCB-II/I ratio and LAMP-1 were determined. On the whole, those results indicated a diminution in the autophagic process in sEHi treated mice. Besides, like a pursuing change in autophagy, EV-UB-52 reduced caspase-3 protein expression in Npc mice, which is increased in comparison with the Wt mice group (Figs 5D, G).

The neuroprotective effects of sEH inhibition was determined by measuring synaptic markers such as synaptophysin (SYN) and postsynaptic density 95 (PSD95). In both cases, Npc mice presented reduced levels compared to the Wt group (Figs 5E-G). As expected, UB-EV-52 treatment increased the protein content for SYN and PSD95 in Npc mice (Figs 5E-G).

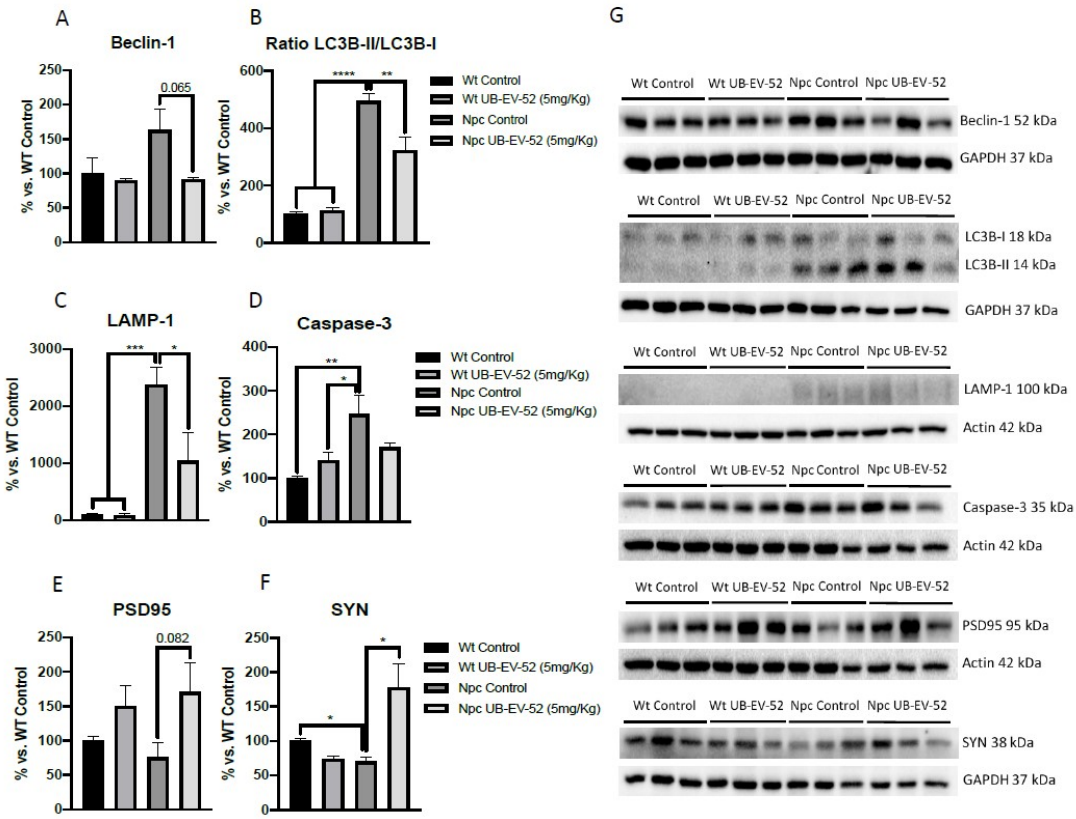

Figure 5. Quantifications and representative Western Blot for Beclin-1 (A-G), ratio LC3B-II/LC3B-I (B-G), LAMP-1 (C-G), Caspase-3 (D-G), PSD95 (E-G) and SYN (F-G) from brain tissue in both females and males. Values in bar graphs are adjusted to 100% for protein levels of the Wt Control. Values are the mean ± Standard error of the mean (SEM); (n = 6 for each group). *p<0.05; **p<0.01.

3. Discussion

Despite various treatment approaches, only modest clinical improvements have been reached for treating the NPC disease. Consequently, its treatment is an unmet clinical need, being necessary to explore new therapeutic strategies [8]. This study focuses on establishing a relationship among cognitive improvement, the anti-inflammatory and anti-oxidant effects and reducing the autophagic process in the brain of the Npc mouse model after UB-EV-52 treatment, a well-known, potent and specific sEHi [21]. We evaluated the impact of sEH pharmacological inhibition on NPC phenotypic characteristics as lipid accumulation, cognitive impairment and other health parameters as weight gain/loss and survival. Targeting the sEH pathway led to an increase in EETs that elicited an anti-inflammatory action that triggers a cascade of molecular and cellular events as modulation of OS, mitochondrial function, ER stress or autophagic process [32,33].

Of paramount importance, oral treatment with UB-EV-52 increased by 25% Npc mice's lifespan, improved weight gain, and reduced the tremor and unstable gait symptoms that were visually detectable in Npc mice in the seventh postnatal week. In addition, motor behaviour and cognition differences were determined at earlier stages (5^{th} to 8^{th} week) [31]. Accordingly, we observed those previously described changes as earlier as weaning time (21 postnatal days), and they were corroborated by the OF and EPM tests. Likewise, sEHi treatment ameliorated locomotor activity as well as reduced some anxiety-like readouts as rearings, or the time that mice spend in open arms in the EPM test. Cognitive impairment is also a severe symptom in the NPC pathology that was addressed after sEHi treatment. UB-EV-52 treatment prevented the cognitive impairment characteristic for the Npc mice model, demonstrated by the elevated DI obtained in the NORT test, both at the short- and long-term. Due to the EV-UB-52 treatment achieved successful rescue of behavioral and cognitive alteration in the NPC mouse model, we focused on the cellular and molecular mechanisms, which participate in the positive action induced by sEHi.

Many neurodegenerative diseases share atypical inflammatory and OS processes as two major pathological events [34]. Thus, this study's particular important insight was to demonstrate that the Npc mice model had a significant increase in gene expression for inflammatory markers such as *Il-1β*, *Tnf-α* that were prevented after sEHi treatment (Fig 4A-B). Inflammation determined spread to brain tissue inducing a significant increase in *Mcp1* and *Gfap*, reflecting the presence of astrogliosis in Npc mice that was also rescued after UB-EV-52 treatment (Fig 4C-D). In summary, these results reinforce the hypothesis that the increase in endogenous anti-inflammatory EETs reduced the disease progression in Npc mice model. Conversely, when we went through OS markers *Hmox1* and *iNOS*, although slight changes were determined in the Npc mice compared to the Wt group, they were not statistically significant. However, OS parameters were partially modified by sEHi treatment. Those results indicated that in the Npc mice model used, OS has not a key role in the disease pathology. In any case, there is evidence that OS is an actor present in humans and most animal models for this illness and production of reactive oxygen species were prevented by α-Tocopherol [35,36]. Therefore, it is plausible that sEHi recovered cellular processes homeostasis, impacting OS parameters positively after UB-EV-52 in our Npc mice model. Of note, UB-EV-52 and other sEHi have also been shown beneficial effects on different mouse models for neurodegenerative or metabolic diseases [21,33].

Pathological processes leading to neurodegeneration in many lysosomal storage disorders are due to the imbalance between induction and autophagy inhibition [37,38]. Concretely, NPC1 deficiency is characterized by increasing the autophagic process inducing increases in ubiquitinated proteins accumulation in the mutant mouse brain [15]. Thus,

 doi:10.20944/preprints202103.0205.v1

several authors have reported similar findings confirming autophagy induction in the NPC brain, liver or primary human fibroblasts from NPC patients. Induction of autophagy and increased Beclin-1 levels are similarly observed in NPC2 deficient primary human fibroblasts and in a chemical model that induces accumulation of unesterified cholesterol by U18666A [39]. Accordingly, we found an increase in Beclin-1 protein levels in our Npc mice model, as well as the inhibition of sEH by UB-EV-52 was able to reduce Beclin-1 protein levels. Those results indicated that although no remarkable changes were delivered in lipid content, sEH inhibition promoted autophagy reduction in the neuronal tissue of the NPC murine model.

Moreover, several studies showed that LC3 levels are not modified by inhibition of lysosome function in pathological situations characterized by impaired autophagosome-lysosome fusion, but the ratio among LC3B-I and -II ratio changes [40]. Consistent with this point, we have found an increase in LC3B-II form compared to LC3B-I, thereby increasing II/I ratio that demonstrated an autophagy activation. Npc mice treated with UB-EV-52 inverted the II/I rate, indicating a reversion in the autophagic process, which positively impacted the disease's progression, as demonstrated phenotypic outcomes presented above (Fig 5B).

To further study the autophagy abnormalities in Npc mice model used and the sEHi treatment's impact, we determined LAMP1 protein levels. LAMP1 is a lysosomal protein implicated macroautophagy process's finalization by the autophagolysosome formation, allowing the initiation of lysosomal activity to degrade proteins, among others [41,42]. Regarding NPC, LAMP1 is associated with cholesterol trafficking into cells and the lysosome, hereby with NPC's etiopathology. LAMP1 overexpression in HeLa cells rescued U18666A-induced cholesterol accumulation and reduced LAMP1 levels based on cyclodextrin's beneficial pharmacological action [39]. Recent studies demonstrated a highly glycosylated form of LAMP1 in NPC1 mice model that correlated neuron loss [43]. A significant increase in LAMP1 protein levels was found in Npc mice, according to Beclin-1 and LC3B ratio observed changes, hereby pointing out the completion of the autophagic process in this model. Of note, sEHi treatment strongly reduced LAMP1 and caspase-3 protein levels, supporting the positive pharmacological effect of UB-EV-52 on the autophagy and apoptotic signaling pathway in this Npc mice model (Figs 5C-D). Although, in our hands, cholesterol levels are not dramatically changed after UB-EV-52 treatment, a slight effect was observed. Therefore, the effect of sEHi in cholesterol trafficking into the lysosome mediated by LAMP1 cannot be discarded, and it can be considered a secondary mechanism to explain the beneficial effects of increasing EETs levels by sEH inhibition.

Lastly, another characteristic feature of NPC disease is the synaptic plasticity abnormalities, promoting memory impairment and dementia [44]. Here, we found reduced levels in the synaptic markers between the Npc control group and the Wt group, being significant for SYN. Furthermore, significant changes in the synaptic marker SYN and, in the same way, a clear tendency for PSD95 in the brain between Npc treated mice groups and Npc controls, demonstrating the neuroprotective effects under sEH inhibition treatment. Consistent with these results, several studies described changes in the levels of synaptic proteins such as Syntaxin-1A, Amphiphysin, Complexin-1, SYN, PSD-95, among others, in lysosomal storage diseases such as NPC disease [45]. Likewise, those observations regarding the sEHi treatment are in agreement with previous reports that demonstrated long-term administration of TPPU, a well-characterized sEHi, to the 5xFAD mouse model of AD also rescued SYN and PSD95 levels [46], suggesting that the improvement in synaptic plasticity and cognitive performance in Npc mice model could be attributed to sEH inhibition.

4. Conclusions

Our results strengthen the inhibition of sEH as a promising therapeutic approach for NPC disease. Thus, we have shown positive rescue of the NPC mouse model phenotype, ameliorating survival and motor activity, as well as cognitive outcomes. Regarding biochemical and molecular disturbances determined, those were modified by the inhibition of the sEH by using a blood-brain barrier (BBB) permeable, oral disposable, potent and specific inhibitor, UB-EV-52. Apart from the anti-inflammatory effect observed after sEHi treatment, OS changes, jointly with autophagy modulation, lipid storage modifications and synaptic plasticity improvement were demonstrated. In the future, more studies are needed to unravel the involvement of sEH in the beneficial effects seen in phenotype and cognition.

5. Materials and Methods

5.1.Animals

Animals used were generated by Gómez-Grau et al. [31]; in brief, the heterozygous *Npc1*$^{imagine/+}$ and *Npc1*$^{pioneer/+}$ mice have a C57BL/6 genetic background, and were kindly given to us for this study by the Addi and Cassi Fund (http://addiandcassi.com/) after generation by the Ozgene company. Heterozygous *Npc1*$^{imagine/+}$ mice were interbred and generated litters consisting of *Npc1*$^{imagine/imagine}$, *Npc1*$^{imagine/+}$ and *Npc1*$^{+/+}$ mice. Heterozygous *Npc1*$^{pioneer/+}$ mice were interbred and generated litters consisting of *Npc1*$^{pioneer/pioneer}$, *Npc1*$^{pioneer/+}$ and *Npc1*$^{+/+}$ mice. We used homozygotes for imagine and pioneer mutation, and up to now, we referred to mutant animals as Npc mice to simplify reading, whereas we used non-mutant littermates as wild-type (Wt) controls. Genotype analysis was performed as describes previously by Gómez-Grau et al.[31].

Animals had free access to food and water and were kept under standard temperature conditions (22±2°C) and 12h: 12h light-dark cycles (300lux/0 lux).

Wt and Npc mice (n=48) were used to perform the cognitive tests followed by the molecular analysis. The animals were randomly divided into four groups: Wild-type (Wt) group (n=12; females n=6; males n=6), Npc (Npc) group (n=12; females n=6; males n=6), Wt treated with UB-EV-52 (Wt UB-EV-52) group (n=12; females n=6; males n=6), and Npc treated with UB-EV-52 (Npc UB-EV-52) group (n=12; females n=6; males n=6). For survival experiment Npc mice (n=24; females n=12; males n=12) were used randomly divided into two groups: Npc (Npc) group (n=12; females n=6; males n=6), and Npc treated with UB-EV-19 (Npc UB-EV-52) group (n=12; females n=6; males n=6).

UB-EV-52 was dissolved in 2% polyethylene glycol 400 (PEG400) at 5 mg/kg/day and administered through drinking water since the weaning (1-month-old). Control groups received also the vehicle into drinking water After four weeks of treatment, behavioral tests were performed on the animals and the drug was administered up to sacrifice. For survival assay, two groups were established Npc (Npc) group (n=12), and Npc treated with UB-EV-52 (Npc UB-EV-52) group (n=12), and UB-EV-52 was administered through drinking water from the weaning (1-month-old) up to natural death. Water consumption was controlled each week and concentrations were adjusted accordingly to reach the optimal dose for each cage.

Studies were performed by the Institutional Guidelines for the Care and Use of Laboratory Animals established by (European Communities Council Directive 2010/63/EU and Guidelines for the Care and Use of Mammals in Neuroscience and Behavioral Research, National Research Council 2003) and were approved by the Animal Experimentation Ethics Committee (CEEA) at the University of Barcelona. All efforts were made to reduce the number of animals and their suffering.

 doi:10.20944/preprints202103.0205.v1

5.2.Cognitive Tests

5.2.1. Open field

The open field test (OFT) is an experiment used to assay general locomotor activity and anxiety in rodents. The test is based on the fear and anxiety of rodents to be in open and luminous spaces. The OFT apparatus was a white polywood box (50x50x25 cm). The arena was divided into two areas defined as center and peripheral zone (15 cm between center zone and the wall). Trials were recorded for later analysis, by using a camera situated above the apparatus and changes in movements were scored with SMART® ver.3.0 software. Each trial started by placing mice at the center and allowing them to explore the box for 5 minutes. The trial ended by returning mice to cages. Between trials, OFT apparatus was carefully cleaned (swipe embedded with 70% ethanol). The parameters scored included center staying duration, rearings and the distance travelled, calculated as the sum of total distance travelled in 5 minutes.

5.2.2.Elevated Plus Maze

The elevated plus maze (EPM) test is based on mice preference for dark enclosed places, and thereby it evaluates anxiety-related and risk-taking behaviours. EPM apparatus consists of 2 opened, and 2 closed arms elevated 50 cm from the floor. Mice were placed on the central platform, facing opened arms, and allowed to explore the apparatus for 5 min. After that, mice were returned to their home cages, and EPM arms were cleaned with 70% ethanol to avoid any olfactory clues. Behaviour was scored with SMART® ver. 3.0 software and each trial were recorded for later analysis. Parameters evaluated included time spent on opened and closed arms, rearings, defecation and urination.

5.2.3.Novel Object Recognition Test

The novel object recognition test (NORT) is a cognitive test used to assess short- and long-term recognition memories. The apparatus used consisted of a 90º, two-arm, 25-cm-long, 20-cm-high, and a 5-cm-wide black maze of black polyvinyl chloride. The objects to be discriminated were made of plastic and chosen not to frighten mice without any part likely to be bitten. The test was performed for 5 days, and the first three days, animals were individually habituated to the apparatus for 10 min. The fourth day, the animals were individually exposed during 10 min to the apparatus and freely explored the zone inside the apparatus (First trial/Familiarization) where we placed two identical novel objects (A+A' or B+B') at the end of each arm. After 10 min, the animals were removed and returned to their home cage, and 2h later the retention trial (second trial) was performed. In the second trial, objects A' and B' were swapped (A+B' or A'+B) and the mice were allowed to explore the maze for 10 min. Twenty-four hours later of the first trial, animals were exposed again to the apparatus, and in this case objects A' and B' were substituted by two new objects with different shapes and colours (A+C or B+C'), and animals were allowed to explore them during 10 min. The time exploring the novel object (TN) and the old object (TO) were measured with a camera and videos were recorded. Exploration of an object was defined as pointing the nose towards the object at a distance ≤2 cm and/or touching it with the nose. Turning or sitting around the object was not considered exploration. To avoid object preference biases objects A and B were counterbalanced so that one-half of the animals in each experimental group were first exposed to object A and then to object B, whereas the other half first saw object B and then object A. Finally, to obtain cognitive performance, the discrimination index (DI) was calculated, which is defined as (TN-TO)/(TN+TO).

5.2.4.Object location test (OLT)

The object location test (OLT) is a well-established task based on the spontaneous tendency of rodents to spend more time exploring a novel object location than a familiar

object location, as well as to recognize when an object has been relocated. The test was carried out for 3 days in a wooden box (50 x 50 x 25 cm), in which three walls were white except one that was black. The first day, the box was empty, and the animals just habituated to the open field arena for 10 minutes. The second day, two objects were placed in front of the black wall, equidistant from each other and the wall. The objects were 10-cm high and identical. The animals were placed into the open field arena and allowed to explore both objects and surroundings, for 10 minutes. Afterwards, animals were returned to their home cages, and the OLT apparatus was cleaned with 70% ethanol. On the third day, one object was moved in front of the white wall to test the spatial memory. Trials were recorded using a camera mounted above the open field area, and the total exploration time was determined by scoring the amount of time (seconds) spent sniffing the object in the new location (TN) and the object in the old location (TO). To evaluate the cognitive performance, the DI was calculated, which is defined as (TN-TO)/(TN+TO).

5.3. Tissues Preparation

After three days of the cognitive and memory tests, all mice groups were euthanized, tissues (liver and brain) isolated and frozen in powdered dry ice and stored at -80°C for further use.

5.4.Protein Level Determination by Western Blotting

For protein extraction, tissue samples were homogenized in lysis buffer containing phosphatase and protease inhibitors (Cocktail II, Sigma-Aldrich). Total protein levels were obtained, and protein concentration was determined by the method of Bradford. 15 μg of protein samples were separated by Sodium dodecyl sulphate-Polyacrylamide gel electrophoresis (SDS-PAGE) (8-20%) and transferred onto Polyvinylidene difluoride (PVDF) membranes (Millipore). Afterwards, membranes were blocked in 5% non-fat milk in Tris-buffered saline (TBS) solution containing 0.1% Tween 20 TBS (TBS-T) for 1 hour at room temperature, followed by overnight incubation at a 4°C with the primary antibodies listed in Table 3. Then, membranes were washed and incubated with secondary antibodies for 1 hour at room temperature. Immunoreactive proteins were viewed with the chemiluminescence-based detection kit, following the manufacturer's protocol (ECL Kit, Millipore), and digital images were acquired using ChemiDoc XRS+ System (BioRad). Semi-quantitative analyses were done using ImageLab software (BioRad), and results were expressed in Arbitrary Units (AU), considering control protein levels as 100%. Protein loading was routinely monitored by immunodetection of Glyceraldehyde-3-phosphate dehydrogenase (GAPDH).

5.5. RNA Extraction and Gene Expression Determination

Total RNA isolation from tissue samples was carried out using TRIsure™ reagent following the manufacturer's instructions (Bioline Reagent). The yield, purity, and quality of RNA were determined spectrophotometrically with a NanoDrop™ ND-1000 (Thermo Scientific) apparatus and an Agilent 2100B Bioanalyzer (Agilent Technologies). RNAs with 260/280 ratios and RIN higher than 7.5, respectively, were selected. Reverse transcription-polymerase chain reaction (RT-PCR) was performed as follows: 2 μg of messenger RNA (mRNA) was reverse-transcribed using the High-Capacity cDNA Reverse Transcription kit (Applied Biosystems). Real-time quantitative PCR (qPCR) was used to quantify the mRNA expression of inflammatory and OS markers genes listed in Table 4.

SYBR® Green real-time PCR was performed on a Step One Plus Detection System (Applied-Biosystems) employing SYBR® Green PCR Master Mix (Applied-Biosystems). Each reaction mixture contained 6.75 μL of complementary DNA (cDNA) (which concentration was 2 μg), 0.75 μL of each primer (which concentration was 100 nM), and 6.75 μL of SYBR® Green PCR Master Mix (2X).

 doi:10.20944/preprints202103.0205.v1

Data were analyzed utilizing the comparative Cycle threshold (Ct) method (ΔΔCt), where the housekeeping gene level was used to normalize differences in sample loading and preparation. Normalization of expression levels was performed with *β-actin* for SYBR® Green-based real-time PCR results. Each sample was analyzed in duplicate, and the results represent the n-fold difference of the transcript levels among different groups.

5.6.Cholesterol measurement

Liver and brain tissue was homogenized using *TissueRuptor (QIAGEN) in PBS at 5% w/v.* Lipids were extracted with a chloroform:methanol (2:1) mixture containing stigmasterol as the internal standard. Samples were derivatised with N,O-Bis(trimethylsilyl) trifluoroacetamide (BSTFA) to form the trimethylsilyl derivatives and analyzed by gas chromatography-mass spectrometry. Gas chromatography coupled to electron impact (70 eV) mass spectrometry was carried out using a Fisons gas chromatograph (8000 series) coupled to a Fisons MD-800 mass-selective detector. The system was equipped with an HP-5-MS capillary column (30 m × 0.20 mm inner diameter), which was programmed to increase from 120°C to 315°C, at 5°C/minute after an initial delay of 2 minutes. Analyses were performed in the selected ion-monitoring mode. The ions selected were those at m/z 129, 458 and 484.

5.7.Sphingolipid determination

Liver and brain tissue were homogenized using TissueRuptor (QIAGEN) in 0.2 M sucrose at 5% w/v. Protein concentration was determined by the Lowry method and a 400μg protein aliquot used for sphingolipid quantification. Sphingolipid extracts, fortified with internal standards, were prepared and different groups of lipids, including ceramides, sphingomyelins, and glycosphingolipids, were analyzed by liquid chromatography-mass spectrometry (LC/MS). The LC/MS analysis consisted of a Waters Acquity UPLC system connected to a Waters LCT Premier orthogonal accelerated time-of-flight mass spectrometer (Waters), operated in positive and negative electrospray ionisation modes. Full scan spectra from 50 to 1500 Da were acquired, and individual spectra were summed to produce data points every 0.2 seconds. Mass accuracy and reproducibility were maintained using an independent reference spray via the LockSpray interference. The analytical column was a 1.7-μ m ethylene-bridged hybrid (C8 Acquity UPLC column, Waters), measuring 100 × 2.1 mm (inner diameter). The two mobile phases were MeOH:HCOOH (998:2, v/v) for phase A and water:HCOOH (998:2, v/v) for phase B, both containing 2 mM ammonium formate. The column was maintained at 30°C. Quantification was carried out using the extracted ion chromatogram of each compound, using 50-mDa windows. The linear dynamic range was determined by injecting standard mixtures. The positive identification of compounds was based on accurate mass measurement with an error of < 5 ppm and its LC retention time, compared with that of a standard (± 2%).

5.8.Data Acquisition and Statistical Analysis

Data analysis was conducted using GraphPad Prism ver. 8 statistical software. Data are expressed as the mean ± standard error of the mean (SEM) of at least 3 samples per group. Strain and treatment effects were compared using the Two-Way analysis of variance (ANOVA), followed by Tukey post-hoc analysis or two-tail Student's t-test when it was necessary. Statistical significance was considered when p-values were <0.05. The statistical outliers were determined with Grubbs' test and when necessary, were removed from the analysis. The cognitive analysis was performed blindly, the person who evaluated videos was different from the person who made the cognitive tests. Furthermore, videos are named with a blind code to avoid analysis bias.

Supplementary Materials: Supplementary Figure 1: Brain lipid storage in sphingomyelin **(A)**, dihydrosphingomyelin **(B)**, ceramide **(C)**, glangliosides **(D)** and cholesterol **(E)** in both females and

males. Data are expressed as mean ± Standard error of the mean (SEM). *p<0.05; **p<0.01; ***p<0.001. **Supplementary Figure 2:** Liver lipid storage in sphingomyelin **(A)**, dihydrosphingomyelin **(B)**, ceramide **(C)**, glangliosides **(D)** and cholesterol **(E)** in both females and males. Data are expressed as mean ± Standard error of the mean (SEM). *p<0.05; **p<0.01; ****p<0.0001. **Table 1.** Parameters measured in the open field test (OFT) in both females and males. (n): number of events. Results are expressed as a mean ± Standard error of the mean (SEM). **p <0.01; ****p <0.0001 vs Wt Control. #p <0.05 vs Npc Control. **Table 2.** Parameters measured in the elevated plus maze Test (EPM) in both females and males. (n): number of events. Results are expressed as a mean ± Standard error of the mean (SEM). **p <0.01; ***p<0.001; ****p <0.0001 vs Wt Control. #p <0.05; ##p <0.01 vs Npc Control **Table 3.** Antibodies used in Western blot studies. **Table 4.** Primers and probes used in qPCR studies.

Author Contributions: Conceptualization, C.G.-F., S.V., D.O.-S., L.V., D.G. and M.P.; methodology, C.G.-F., J.C.A., S.C.; formal analysis, C.G.-F.; data curation, C.G.-F. and J.C.A.; writing—original draft preparation, C.G.-F. and M.P.; writing—review and editing, S.V., D.O.-S.; L.V., D.G; supervision, S.V., L.V., D.G. and M.P.; project administration, C.G.-F. and M.P.; funding acquisition, C.G.-F., S.V. and M.P.

Funding: This study has been co-financed by Secretaria d'Universitats i Recerca del Departament d'Empresa i Coneixement de la Generalitat de Catalunya 2018 (Llavor 00007); by Ministerio de Economía y Competitividad of Spain (SAF2016-77703 and PID2019-106285RB) and by the European Regional Development Fund (FEDER). C.G.-F., S.C., S.V. and M.P. belong to 2017SGR106 (AGAUR, Catalonia). Financial support was provided for J.C.A. (FI program).**Acknowledgments:** In this section, you can acknowledge any support given which is not covered by the author contribution or funding sections. This may include administrative and technical support, or donations in kind (e.g., materials used for experiments).

Conflicts of Interest: The authors declare no conflict of interest. The funders had no role in the study's design; in the collection, analyses, or interpretation of data; in the writing of the manuscript, or in the decision to publish the results.

References

1. Vanier, M.T.; Millat, G. Niemann–Pick disease type C. *Clin. Genet.* **2003**, *64*, 269–281.
2. Vanier, M.T. Complex lipid trafficking in Niemann-Pick disease type C. *J. Inherit. Metab. Dis.* **2015**, *38*, 187–199.
3. Torres, S.; Matías, N.; Baulies, A.; Nuñez, S.; Alarcon-Vila, C.; Martinez, L.; Nuño, N.; Fernandez, A.; Caballeria, J.; Levade, T. Mitochondrial GSH replenishment as a potential therapeutic approach for Niemann Pick type C disease. *Redox Biol.* **2017**, *11*, 60–72.
4. Rosenbaum, A.I.; Maxfield, F.R. Niemann-Pick type C disease: molecular mechanisms and potential therapeutic approaches. *J. Neurochem.* **2011**, *116*, 789–795.
5. Evans, W.R.H.; Hendriksz, C.J. Niemann-Pick type C disease–the tip of the iceberg? A review of neuropsychiatric presentation, diagnosis and treatment. *BJPsych Bull.* **2017**, *41*, 109–114.
6. Walterfang, M.; Fietz, M.; Fahey, M.; Sullivan, D.; Leane, P.; Lubman, D.I.; Velakoulis, D. The neuropsychiatry of Niemann-Pick type C disease in adulthood. *J. Neuropsychiatry Clin. Neurosci.* **2006**, *18*, 158–170.
7. Distl, R.; Treiber-Held, S.; Albert, F.; Meske, V.; Harzer, K.; Ohm, T.G. Cholesterol storage and tau pathology in Niemann–Pick type C disease in the brain. *J. Pathol. A J. Pathol. Soc. Gt. Britain Irel.* **2003**, *200*, 104–111.
8. Bräuer, A.U.; Kuhla, A.; Holzmann, C.; Wree, A.; Witt, M. Current Challenges in Understanding the Cellular and Molecular Mechanisms in Niemann–Pick Disease Type C1. *Int. J. Mol. Sci.* **2019**, *20*, 4392.
9. Malnar, M.; Hecimovic, S.; Mattsson, N.; Zetterberg, H. Bidirectional links between Alzheimer's disease and Niemann–Pick type C disease. *Neurobiol. Dis.* **2014**, *72*, 37–47.
10. Papassotiropoulos, A.; Streffer, J.R.; Tsolaki, M.; Schmid, S.; Thal, D.; Nicosia, F.; Iakovidou, V.; Maddalena, A.; Lütjohann,

D.; Ghebremedhin, E. Increased brain β-amyloid load, phosphorylated tau, and risk of Alzheimer disease associated with an intronic CYP46 polymorphism. *Arch. Neurol.* **2003**, *60*, 29–35.

11. Codogno, P.; Meijer, A.J. Autophagy and signaling: their role in cell survival and cell death. *Cell Death Differ.* **2005**, *12*, 1509–1518.
12. Nikoletopoulou, V.; Papandreou, M.E.; Tavernarakis, N. Autophagy in the physiology and pathology of the central nervous system. *Cell Death Differ.* **2015**, *22*, 398–407.
13. Yamamoto, A.; Yue, Z. Autophagy and its normal and pathogenic states in the brain. *Annu. Rev. Neurosci.* **2014**, *37*, 55–78.
14. Pacheco, C.D.; Elrick, M.J.; Lieberman, A.P. Tau deletion exacerbates the phenotype of Niemann–Pick type C mice and implicates autophagy in pathogenesis. *Hum. Mol. Genet.* **2009**, *18*, 956–965.
15. Pacheco, C.D.; Kunkel, R.; Lieberman, A.P. Autophagy in Niemann–Pick C disease is dependent upon Beclin-1 and responsive to lipid trafficking defects. *Hum. Mol. Genet.* **2007**, *16*, 1495–1503.
16. Hammond, N.; Munkacsi, A.B.; Sturley, S.L. The complexity of a monogenic neurodegenerative disease: More than two decades of therapeutic driven research into Niemann-Pick type C disease. *Biochim. Biophys. Acta (BBA)-Molecular Cell Biol. Lipids* **2019**, *1864*, 1109–1123.
17. Kulkarni, A.; Caporali, P.; Dolas, A.; Johny, S.; Goyal, S.; Dragotto, J.; Macone, A.; Jayaraman, R.; Fiorenza, M.T. Linear Cyclodextrin Polymer Prodrugs as Novel Therapeutics for Niemann-Pick Type C1 Disorder. *Sci. Rep.* **2018**, *8*, 1–13.
18. Smith, D.; Wallom, K.-L.; Williams, I.M.; Jeyakumar, M.; Platt, F.M. Beneficial effects of anti-inflammatory therapy in a mouse model of Niemann-Pick disease type C1. *Neurobiol. Dis.* **2009**, *36*, 242–251.
19. Maass, F.; Petersen, J.; Hovakimyan, M.; Schmitt, O.; Witt, M.; Hawlitschka, A.; Lukas, J.; Rolfs, A.; Wree, A. Reduced cerebellar neurodegeneration after combined therapy with cyclodextrin/allopregnanolone and miglustat in NPC1: A mouse model of Niemann-Pick type C1 disease. *J. Neurosci. Res.* 2015, 93, 433–442.
20. Lyseng-Williamson, K.A. Miglustat: a review of its use in Niemann-Pick disease type C. *Drugs* **2014**, *74*, 61–74.
21. Iyer, A.; Kauter, K.; Alam, M.; Hwang, S.H.; Morisseau, C.; Hammock, B.D.; Brown, L. Pharmacological inhibition of soluble epoxide hydrolase ameliorates diet-induced metabolic syndrome in rats. *Exp. Diabetes Res.* **2011**, *2012*.
22. Griñán-Ferré, C.; Codony, S.; Pujol, E.; Yang, J.; Leiva, R.; Escolano, C.; Puigoriol-Illamola, D.; Companys-Alemany, J.; Corpas, R.; Sanfeliu, C. Pharmacological inhibition of soluble epoxide hydrolase as a new therapy for Alzheimer's disease. *Neurotherapeutics* **2020**, 7(4):1825-1835.
23. Lee, H.-T.; Lee, K.-I.; Chen, C.-H.; Lee, T.-S. Genetic deletion of soluble epoxide hydrolase delays the progression of Alzheimer's disease. *J. Neuroinflammation* **2019**, *16*, 1–12.
24. Pallàs, M.; Vázquez, S.; Sanfeliu, C.; Galdeano, C.; Griñán-Ferré, C. Soluble epoxide hydrolase inhibition to face neuroinflammation in Parkinson's disease: A new therapeutic strategy. *Biomolecules* **2020**, *10*, 703.
25. Morisseau, C.; Hammock, B.D. Impact of soluble epoxide hydrolase and epoxyeicosanoids on human health. *Annu. Rev. Pharmacol. Toxicol.* **2013**, *53*, 37–58.
26. Sarkar, P.; Zaja, I.; Bienengraeber, M.; Rarick, K.R.; Terashvili, M.; Canfield, S.; Falck, J.R.; Harder, D.R. Epoxyeicosatrienoic acids pretreatment improves amyloid β-induced mitochondrial dysfunction in cultured rat hippocampal astrocytes. *Am. J. Physiol. Circ. Physiol.* **2014**, *306*, H475–H484.
27. Geng, H.-X.; Li, R.-P.; Li, Y.-G.; Wang, X.-Q.; Zhang, L.; Deng, J.-B.; Wang, L.; Deng, J.-X. 14, 15-EET suppresses neuronal apoptosis in ischemia–reperfusion through the mitochondrial pathway. *Neurochem. Res.* **2017**, *42*, 2841–2849.
28. López-Vicario, C.; Alcaraz-Quiles, J.; García-Alonso, V.; Rius, B.; Hwang, S.H.; Titos, E.; Lopategi, A.; Hammock, B.D.; Arroyo, V.; Clària, J. Inhibition of soluble epoxide hydrolase modulates inflammation and autophagy in obese adipose tissue and liver: role for omega-3 epoxides. *Proc. Natl. Acad. Sci.* **2015**, *112*, 536–541.
29. Schmelzer, K.R.; Kubala, L.; Newman, J.W.; Kim, I.-H.; Eiserich, J.P.; Hammock, B.D. Soluble epoxide hydrolase is a

therapeutic target for acute inflammation. *Proc. Natl. Acad. Sci.* **2005**, *102*, 9772–9777.

30. Wang, L.; Luo, G.; Zhang, L.-F.; Geng, H.-X. Neuroprotective effects of epoxyeicosatrienoic acids. *Prostaglandins Other Lipid Mediat.* **2018**, *138*, 9–14.
31. Kang, I.; Lee, B.-C.; Lee, J.Y.; Kim, J.-J.; Sung, E.-A.; Lee, S.E.; Shin, N.; Choi, S.W.; Seo, Y.; Kim, H.-S. Stem cell-secreted 14, 15-epoxyeicosatrienoic acid rescues cholesterol homeostasis and autophagic flux in Niemann–Pick-type C disease. *Exp. Mol. Med.* **2018**, *50*, 1–14.
32. Gómez-Grau, M.; Albaigès, J.; Casas, J.; Auladell, C.; Dierssen, M.; Vilageliu, L.; Grinberg, D. New murine Niemann-Pick type C models bearing a pseudoexon-generating mutation recapitulate the main neurobehavioural and molecular features of the disease. *Sci. Rep.* **2017**, *7*, 1–16.
33. Shen, H.C.; Hammock, B.D. Discovery of inhibitors of soluble epoxide hydrolase: a target with multiple potential therapeutic indications. *J. Med. Chem.* **2012**, *55*, 1789–1808.
34. Wagner, K.M.; McReynolds, C.B.; Schmidt, W.K.; Hammock, B.D. Soluble epoxide hydrolase as a therapeutic target for pain, inflammatory and neurodegenerative diseases. *Pharmacol. Ther.* **2017**, *180*, 62–76.
35. Fischer, R.; Maier, O. Interrelation of oxidative stress and inflammation in neurodegenerative disease: role of TNF. *Oxid. Med. Cell. Longev.* **2015**, *2015*.
36. Narushima, K.; Takada, T.; Yamanashi, Y.; Suzuki, H. Niemann-Pick C1-like 1 mediates α-tocopherol transport. *Mol. Pharmacol.* **2008**, *74*, 42–49.
37. Xu, M.; Liu, K.; Swaroop, M.; Porter, F.D.; Sidhu, R.; Finkes, S.; Ory, D.S.; Marugan, J.J.; Xiao, J.; Southall, N. δ-Tocopherol reduces lipid accumulation in Niemann-Pick type C1 and Wolman cholesterol storage disorders. *J. Biol. Chem.* **2012**, *287*, 39349–39360.
38. Settembre, C.; Fraldi, A.; Rubinsztein, D.C.; Ballabio, A. Lysosomal storage diseases as disorders of autophagy. *Autophagy* **2008**, *4*, 113–114.
39. Ward, C.; Martinez-Lopez, N.; Otten, E.G.; Carroll, B.; Maetzel, D.; Singh, R.; Sarkar, S.; Korolchuk, V.I. Autophagy, lipophagy and lysosomal lipid storage disorders. *Biochim. Biophys. Acta (BBA)-Molecular Cell Biol. Lipids* **2016**, *1861*, 269–284.
40. Lu, F.; Liang, Q.; Abi-Mosleh, L.; Das, A.; De Brabander, J.K.; Goldstein, J.L.; Brown, M.S. Identification of NPC1 as the target of U18666A, an inhibitor of lysosomal cholesterol export and Ebola infection. *Elife* **2015**, *4*, e12177.
41. Tanida, I.; Ueno, T.; Kominami, E. LC3 and Autophagy. In *Autophagosome and phagosome*; Springer, 2008; pp. 77–88.
42. Meikle, P.J.; Brooks, D.A.; Ravenscroft, E.M.; Yan, M.; Williams, R.E.; Jaunzems, A.E.; Chataway, T.K.; Karageorgos, L.E.; Davey, R.C.; Boulter, C.D. Diagnosis of lysosomal storage disorders: evaluation of lysosome-associated membrane protein LAMP-1 as a diagnostic marker. *Clin. Chem.* **1997**, *43*, 1325–1335.
43. Platt, F.M.; Boland, B.; van der Spoel, A.C. Lysosomal storage disorders: The cellular impact of lysosomal dysfunction. *J. Cell Biol.* **2012**, *199*, 723–734.
44. Pará, C.; Bose, P.; Pshezhetsky, A. V. Neuropathophysiology of Lysosomal Storage Diseases: Synaptic Dysfunction as a Starting Point for Disease Progression. *J Clin Med*. 2020; 9(3):616.
45. D'Arcangelo, G.; Grossi, D.; Racaniello, M.; Cardinale, A.; Zaratti, A.; Rufini, S.; Cutarelli, A.; Tancredi, V.; Merlo, D.; & Frank, C. Miglustat Reverts the Impairment of Synaptic Plasticity in a Mouse Model of NPC Disease. *Neural Plast.* 2016; 3830424.
46. Ghosh, A.; Comerota, M.M.; Wan, D.; Chen, F.; Propson, N.E.; Hwang, S.H.; Hammock, B.D.; Zheng, H. An epoxide hydrolase inhibitor reduces neuroinflammation in a mouse model of Alzheimer's disease. *Sci. Transl. Med.* **2020**, *2(573):eabb1206.*